| | |
|---|---|
| File ID | uvapub:19879 |
| Filename | 56047.web.pdf |
| Version | unknown |

SOURCE (OR PART OF THE FOLLOWING SOURCE):

| | |
|---|---|
| Type | article |
| Title | Delayed Nickel Decay in Gamma-Ray Bursts |
| Author(s) | G.C. McLaughlin, R.A.M.J. Wijers |
| Faculty | FNWI: Astronomical Institute Anton Pannekoek (IAP) |
| Year | 2002 |

FULL BIBLIOGRAPHIC DETAILS:
      http://hdl.handle.net/11245/1.197952

# DELAYED NICKEL DECAY IN GAMMA-RAY BURSTS

G. C. McLaughlin

Department of Physics, North Carolina State University, Raleigh, NC 27695-8202; gail_mclaughlin@ncsu.edu

AND

R. A. M. J. Wijers

Department of Physics and Astronomy, State University of New York, Stony Brook, NY 11794-3800; ralph.wijers@sunysb.edu

## ABSTRACT

Recently observed emission lines in the X-ray afterglow of $\gamma$-ray bursts suggest that iron-group elements are either produced in the $\gamma$-ray burst or are present nearby. If this material is the product of a thermonuclear burn, then such material would be expected to be rich in nickel-56. If the nickel remains partially ionized, this prevents the electron capture reaction normally associated with the decay of nickel-56, dramatically increasing the decay timescale. Here we examine the consequences of rapid ejection of a fraction of a solar mass of iron-group material from the center of a collapsar/hypernova. The exact rate of decay then depends on the details of the ionization and, therefore, the ejection process. Future observations of iron, nickel, and cobalt lines can be used to diagnose the origin of these elements and to better understand the astrophysical site of $\gamma$-ray bursts. In this model, the X-ray lines of these iron-group elements could be detected in suspected hypernovae that did not produce an observable $\gamma$-ray burst due to beaming.

*Subject headings:* gamma rays: bursts — line: profiles — nuclear reactions, nucleosynthesis, abundances — supernovae: general

## 1. INTRODUCTION

For the last 30 years, $\gamma$-ray bursts have been observed, but it has only been in the last 5 years that X-ray, optical, and radio counterparts—the afterglows—have been seen (Costa et al. 1997; van Paradijs et al. 1997; Frail et al. 1997). Pinpointing the location of the afterglows has allowed some of the bursts to be associated with host galaxies. Absorption lines in the optical afterglow, together with redshifts obtained from the host galaxies, have allowed redshifts to be obtained for the $\gamma$-ray bursts themselves (Metzger et al. 1997). Redshifts have been obtained between $z = 0.35$ and $z = 4.5$, confirming the idea that bursts are cosmological in origin. This idea is also supported by their isotropic distribution on the sky, as recorded by over 2700 BATSE detections.

The redshift determinations have led to estimates of isotropic equivalent fluxes in $\gamma$-rays, ranging from $10^{50}$ to $10^{54}$ ergs. Since the upper bound is approaching the rest-mass energy of the Sun, the astrophysical origin of these sites is fairly restrictive. Less energy is contained in the bursts if the $\gamma$-rays are strongly beamed, but the beaming cannot be stronger than a few degrees based on the lack of detection of homeless afterglows (Mészáros, Rees, & Wijers 1999; Dalal, Griest, & Pruet 2002; van den Berk et al. 2002; P. M. Vreeswijk et al. 2002, in preparation). Recent analyses of the break in the afterglow signal support the idea that $\gamma$-ray bursts are beamed to a few degrees (Frail et al. 2001; Panaitescu & Kumar 2001).

The theoretical problem of what causes the $\gamma$-ray bursts can be divided into several parts: the fireball model, the energy injection mechanism, and the astrophysical site. The mechanism for actually producing the $\gamma$-rays and the afterglows is described by the relativistic fireball model (Rees & Mészáros 1992; Mészáros & Rees 1997; Wijers, Rees, & Mészáros 1997). After energy is injected into material composed mostly of electrons and positrons, it is ejected relativistically. Internal shocks in the plasma and external shocks caused by contact with the interstellar medium drive synchrotron radiation from the electrons in a magnetic field. The spectrum of the afterglow, at least in some cases, is fairly well fitted to a synchrotron spectrum. For recent reviews, see van Paradijs, Kouveliotou, & Wijers (2000) and Piran (1999).

This model is fairly independent of the initial energy injection mechanism as well as the astrophysical site for the bursts. For the injection mechanism, neutrino and antineutrino annihilation into electron-positron pairs (Ruffert & Janka 1999) and delivery through a pointing flux such as the Blanford-Znajek mechanism have been discussed (Brown et al. 2000).

Two contenders for the site of $\gamma$-ray bursts are neutron star-neutron star mergers and failed supernovae also known as collapsar or hypernova models. The neutron star models (Eichler et al. 1989; Mochkovitch et al. 1993) have been shown to be dependent on the way general relativity is handled in the numerics. Janka (1999), using a post-Newtonian approximation, finds short bursts with, at most, $10^{50}$ ergs ejected. Salmonson, Wilson, & Mathews (2001), using a general relativity approximation that is exact in the case of spherical symmetry, find longer timescales and larger energies. The collapsar models involve the collapse of a massive star that fails to produce a viable shock for an ordinary supernova explosion. Models involve a combination of a rotating black hole and magnetic field driving jets along the rotation axis of the black hole (Woosley 1993; Paczyński 1998; MacFadyen & Woosley 1999). Of these two models, the collapsar model has recently gained favor with the identification, in many cases, of host galaxies associated with the $\gamma$-ray burst (Bulik, Belczynski, & Zbijewski 1999; Bloom, Sigurdsson, & Pols 1999). Neutron star binaries would be expected to wander out of galaxies at a rate inconsistent

with the number of observed associations with host galaxies. Further, in a number of $\gamma$-ray burst light curves, features strongly resembling a supernova have been found.

Furthermore, recent observations of K$\alpha$ lines from iron have been identified in the X-ray afterglows of four $\gamma$-ray bursts (Piro et al. 1999, 2000; Antonelli et al. 2000). This is more likely to occur in a supernova-like model than in the neutron star merger models. However, there are still many unsolved puzzles associated with these lines. The lines are too broad (0.5 keV) to be accounted for by thermal broadening, although this may be accounted for by electron scattering. Line scattering from reprocessor-type models is discussed in, e.g., Weth et al. (2000), McLaughlin et al. (2001), and Kallman et al. (2001). If the lines come from material produced by nucleosynthesis in a $\gamma$-ray burst, then one would expect nickel-56 as the product of a thermonuclear burn. In most cases, the lines have been identified as iron, in some cases, with independent redshift measurements. However, the most recent detection is of nickel, not iron (Reeves et al. 2002).

Two general classes of models have been proposed for these lines. In one case, the iron is assumed to have been formed some time before the $\gamma$-ray burst and is located well outside the blast wave. The $\gamma$-ray burst flash ionizes the iron, which then fluoresces and produces the line (Vietri et al. 2001). In the other case, the iron is produced in a stellar explosion that, at the same time, causes the $\gamma$-ray burst. The blast wave is well outside the iron-rich region and cannot contribute to its ionization. Instead, residual activity of the $\gamma$-ray burst source, such as accretion onto a black hole, produces the X-ray flux. Iron on the wall of the "funnel" carved out of the star by the original explosion is then made to fluoresce by this flux (cf. Rees & Mészáros 2000).

Nickel, on the other hand, is likely to be produced by a thermonuclear burn in the silicon burning layer of the star. This could be identified by a time dependence in the energy of the observed line, due to the decay from nickel to cobalt to iron (McLaughlin et al. 2001). This could, in principle, be detected up to a few days after the event since the half-life for nickel is about 6 days and the difference in line energy from nickel to cobalt is about half a keV. An alternative mechanism suggested for the production of nickel is that, first, material in the very hot accretion disk is completely dissociated into protons and neutrons. A wind from this disk will cool as it moves out and may recombine to an equilibrium nucleus, likely again nickel (McFadyen 2002).

In this paper, we suggest a variation on the above scenarios. Nickel produced by a thermonuclear burn in the silicon shell may be ejected out of the accretion disk surrounding the black hole in the collapsar model. This nickel will be partially ionized from below by the flux leaving the accretion funnel. The ionized nickel will decay at a different rate than nonionized nickel since decay of nickel proceeds by electron capture. This will produce a distinctive signature pattern in the time dependence of recombination lines. In § 2, we make a plausibility argument to show that ejected nickel can remain ionized. We discuss the parameters that determine the optical depth of the ejected nickel. We describe the progress of an ionization front through the ejected nickel and its dependence on various parameters. In § 3, we discuss the relevant nuclear physics of electron capture and beta decay of nickel-56 and cobalt-56. In § 4, we give the fractions of these elements as functions of time in this model. In § 5, we give conclusions.

## 2. THE MODEL

In this section, we present a model of material ejected from a the center of a $\gamma$-ray burst. We assume that this occurs by way of interaction between the rotating accretion disk surrounding a black hole and the magnetic field. If the $\gamma$-ray burst is a collapsar/hypernova, then the material is likely to be rich in nickel-56. This will happen if the silicon burning shell with an electron fraction of roughly 0.5 is heated to $T > 4 \times 10^9$ K. This type of burning occurs in ordinary supernova explosions. Some of this nucleosynthesis may be deposited in the accretion disk. First, we discuss the optical depth of the nickel, and then we describe the motion of an ionization front that travels through the ejected material.

### 2.1. Optical Depth

In this subsection, we describe the optical depth of material ejected with fairly high velocity ($\beta \approx v/c \approx 0.2$) from the center of a $\gamma$-ray burst. There is an ionizing flux coming from the center of the object, presumably from an accretion disk surrounding a black hole. As the material moves away from the center, it also expands, so we approximate its size as roughly $V \sim \Omega r^2 \Delta r$, where $r = \beta c t$, $\Omega = 2\pi(1 - \cos\theta)$, and $\Delta r \approx r$. Here $r$ is the linear dimension, $t$ is time, and $c$ is the speed of light. For definiteness, we assume in our calculations that the expansion is homologous, i.e., $v \propto r$, and that the leading edge moves with $v = \beta c$. This way, the density of the ejecta is independent of position and scales with time as $t^{-3}$. Since the ejecta are highly supersonic and the radiation force is small except near the inner edge, it is fair to approximate the velocity of each part of the ejecta as constant.

We wish to determine how much of the nickel is fully ionized as a function of both position and time. The first step is to estimate the recombination rate and the ionization rate for the expanding material. The ionization rate is given by

$$R_{ion} = \int_{\nu_Z}^{\infty} \sigma(\nu, Z) \frac{F(\nu)}{h\nu} d\nu . \tag{1}$$

We use $\sigma(Z) = 2.8 \times 10^{29} Z^4 / \nu^3$ for the ionization cross section. The lower limit of integration is the binding energy of the final K-shell electron, $h\nu = 13.6 Z^2$ eV, $F(\nu)$ is the photon energy flux.

This flux may have different forms depending on the details of the model. The observed ionizing fluxes are much larger than can be supplied by Eddington-limited emission from a disk around a black hole of a few solar masses. However, a mechanical and/or Poynting wind generated by the Blandford-Znajek mechanism or neutrino annihilation can have a much larger energy flux and be converted into heat and radiation when it impacts the funnel wall far from the black hole (or from a highly magnetized neutron star), as envisaged by Rees & Mészáros (2000). In that case, the expected spectrum might be more like synchrotron radiation or bremsstrahlung with a very high temperature; in both cases, we may approximate the keV X-ray spectrum with a power law, $F(\nu) \propto \nu^{-\xi}$.

This is related to the number flux of the material above the ionization threshold as

$$\dot{N}_I = 4\pi r^2 \int_{h\nu_Z}^{\infty} \frac{F(\nu)}{h\nu} . \tag{2}$$

We parameterize the time dependence of the ionizing source (in $10^{53}$ photons s$^{-1}$) as

$$\dot{N}_I = N_{I,53} t_d^{-\alpha} 10^{53} \text{ s}^{-1} , \qquad (3)$$

where time is measured in days ($t_d$). After some algebra, we rewrite the ionization rate as

$$R_{\text{ion}} = 6.5 \times 10^6 t_d^{-(2+\alpha)} N_{I,53} \left(\frac{0.2}{\beta}\right)^2 \left(\frac{28}{Z}\right)^2 \zeta , \qquad (4)$$

where

$$\zeta = \frac{\int_{\nu_Z}^{\infty} (F_\nu/h\nu)(1/\nu^3) d\nu}{\int_{\nu_Z}^{\infty} (F_\nu/h\nu) d\nu} , \qquad (5)$$

i.e., a form factor expressing the ionizing photon number flux with the cross section above the edge threshold. For a power-law spectrum $F(\nu) \propto \nu^{-\xi}$, we have $\zeta = 4\xi/(\xi+3)$.

Also necessary is the recombination rate, which we estimate by starting with the recombination luminosity (Lang 1980),

$$L_{\text{rec}} = 10^{-21} n_e n_i T^{-1/2} V Z^4 \text{ ergs s}^{-1} . \qquad (6)$$

Here temperature is in kelvins, electron ($n_e$) and ion ($n_i$) densities are in cm$^{-3}$, and $V$ is volume. The recombination rate ion$^{-1}$ can be estimated by dividing by the volume and ion density and also by the energy of the photon, $h\nu \approx Z^2 13.6$ eV. Some algebra yields a recombination rate of

$$R_{\text{rec}} = \frac{C_{\text{rec}}}{t_d^3} \text{ day}^{-1} , \qquad (7)$$

with time ($t$) in days where

$$C_{\text{rec}} = 1.1 \times 10^6 \left(\frac{1 \text{ keV}}{T}\right)^{1/2} \left(\frac{M}{0.1 \ M_\odot}\right)$$
$$\times \left(\frac{0.2}{\beta}\right)^3 \left(\frac{1-\cos 20°}{1-\cos\theta}\right) \left(\frac{Z}{28}\right)^3 \left(\frac{A}{56}\right) . \qquad (8)$$

Here $M$ is the amount of mass in the ejected material and $\theta$ is the opening angle of the cone; $T$ is the temperature of the material.

With the recombination and ionization rates, we can calculate the fraction of nonionized nickel in the optically thin region of the material as

$$f_{\text{non}} = \frac{1}{1 + R_{\text{ion}}/R_{\text{rec}}} = \frac{1}{1 + C_i t_d^{1-\alpha}} , \qquad (9)$$

where the coefficient is

$$C_i \approx 6\dot{N}_{I,53} \left(\frac{1-\cos\theta}{1-\cos 20°}\right) \left(\frac{\beta}{0.2}\right) \left(\frac{0.1 \ M_\odot}{M}\right)$$
$$\times \left(\frac{T}{\text{keV}}\right)^{1/2} \left(\frac{28}{Z}\right)^5 \left(\frac{56}{A}\right) \zeta . \qquad (10)$$

If the luminosity of the ionization source is constant, then the fraction of nonionized nickel decreases with time. This may be counterintuitive since the material gets farther from the ionizing source. But the ionization rate atom per atom decreases with flux, i.e., as $1/r^2 \propto 1/t^2$ (since $r \propto t$), whereas the recombination rate is proportional to density, i.e., scales

as $1/r^3 \propto 1/t^3$; hence, ionization wins. However, in case of an emptying accretion disk or of a spinning-down black hole, the luminosity will scale roughly as $t^{-1}$, which implies a roughly constant ionized fraction.

The optical depth of the ionizing photons, $\tau = f_{\text{non}} n_i \sigma_Z r$, is an decreasing function of time. Therefore, an ionization front passes through the material. The details of this ionization front determine the ratio of ionized to nonionized nickel in the material and, therefore, the rate of nickel decay.

## 2.2. Ionization Front

We assume that nickel-56 is ejected from the accretion disk with fairly high velocity. There is a source of ionizing photons that emits in photons per (unit time),

$$\dot{N} = N_{I,53} 10^{53}/t_d^\alpha \text{ s}^{-1} = C_s N_i/t_d^\alpha \text{ day}^{-1} , \qquad (11)$$

where $N_i$ is the total number of ions in the material ($n_i$ is the number density of ions) and

$$C_s = 4 \times 10^3 \left(\frac{M}{0.1 \ M_\odot}\right)^{-1} \left(\frac{A}{56}\right) N_{I,53} . \qquad (12)$$

The equation that describes the passage of the ionization front is

$$\dot{N}\Delta t = n_i f_{\text{non}} R_{\text{ion}} \Omega r_{\text{max}}^3 r_{f_i}^3 \Delta t + n_i \Omega r_{\text{max}}^3 r_{f_i}^2 \Delta r_{f_i} . \qquad (13)$$

The photons are absorbed either on their way to the front (first term) or at the front (second term). In the spherical case, recombination to the ground state is ignored since it recreates a photon that will ionize another atom. Here, however, we have an elongated volume of material in which the photons all travel in the long direction. A photon that is absorbed will be reemitted isotropically and is most likely to escape the volume sideways before ionizing another atom, even if it is energetically capable of ionizing another atom. Here $r_{\text{max}}$ is the total linear dimension of the ejected material and $r_f = r/r_{\text{max}}$ is the fractional distance within that material, while $r_{f_i}$ is the position of the ionization front. The solid angle subtended by the ejected material is $\Omega = 2\pi(1-\cos\theta)$. We rewrite equation (13) as

$$\frac{3C_s}{t_d^\alpha} \approx \frac{3C_{\text{rec}}}{t_d^3} r_{f_i}^3 + \frac{dr_{f_i}^3}{dt} . \qquad (14)$$

Here we have used the fact that the total volume is equal to $\Omega r^3$ and, therefore, $n_i \Omega = N_i$. We have also used equation (9) in the limit that $R_{\text{rec}} \ll R_{\text{ion}}$. The solution to this equation is

$$r_{f_i} \approx \left(\frac{C_s}{C_{\text{rec}}}\right)^{1/3} t_d^{(3-\alpha)/3} , \qquad (15)$$

as long as $(3C_{\text{rec}}/2)^{1/2} \gg t_d$ during the time the ionization front is passing through the material. This is true for all the situations considered here.

Equation (15) describes the motion of the ionization front for $\alpha < 3$. For larger $\alpha$, the flux declines so fast that the flux does not affect the ionization of the material, at least on long timescales. The time it takes a front to pass through the entire mass of nickel depends strongly on $\alpha$. For example, for the parameters considered here, it takes 6 days for the

front to pass through the material if $\alpha = 0$ and 17 days for the front to pass through if $\alpha = 1$.

We have now described a moving, expanding mass of nickel that is partially ionized behind the front and not ionized ahead of the front. We wish to determine the decay properties of the nickel, for which we need the nuclear physics described in the next section.

## 3. ELECTRON CAPTURE AND BETA DECAY

Here we describe the nuclear physics of the $A = 56$ decay chain. The half-life of $^{56}$Ni is 6.075 days, and it decays almost exclusively by electron capture,

$$^{56}\text{Ni} + e^- \rightarrow {}^{56}\text{Co} + \nu_e \ . \qquad (16)$$

The $Q$-value of this reaction is 2.136 MeV. The decay proceeds primarily through the third and fourth excited states of cobalt-56 that are at 1.45 and 1.720 MeV with respect to the ground state. These states have spin and parity of $0^+$ and $1^+$ while the ground state of nickel is $0^+$, so the decay proceeds through Gamow-Teller and Fermi transitions.

If the nickel is completely ionized and in a dilute environment (so free electron capture is negligible), then it can decay by emission of a positron,

$$^{56}\text{Ni} \rightarrow {}^{56}\text{Co} + e^+ + \nu_e \ . \qquad (17)$$

The $Q$-value for this beta plus decay is 1.114 MeV, which makes the third and fourth excited states in cobalt energetically inaccessible. There are three remaining possibilities. The decay can proceed through the ground state, $4^+$, the first excited state at 0.158 Mev, $3^+$, or the second excited state at 0.970 MeV at $2^+$. These are all forbidden and to date no $\beta^+$ decay from nickel-56 has ever been seen. The current experimental limits place the half-life at greater than $2.9 \times 10^4$ yr (Sur et al. 1990). Calculations within the large-scale shell model have placed the half-life at about $4 \times 10^4$ yr (Fisker et al. 1999). For our purposes, we assume that completely ionized nickel is quasi-stable. We note that because of the long half-life of ionized nickel-56, it has been suggested that it may be seen in cosmic-ray detectors.

Cobalt-56 also decays primarily (81%) by electron capture into iron-56:

$$^{56}\text{Co} + e^- \rightarrow {}^{56}\text{Fe} + \nu_e \ . \qquad (18)$$

Its half-life is 77.2 days (Junde 1999). The $Q$-value, 4.566 MeV, is much higher than in the case of nickel, and therefore it has more energetically accessible states in iron into which it may decay. Nineteen percent of the time ($I_{\beta^+} = 0.19$), cobalt-56 decays by emission of a positron,

$$^{56}\text{Co} \rightarrow {}^{56}\text{Fe} + e^+ + \nu_e \ , \qquad (19)$$

the majority of which is a $4^+$ to $4^+$ transition to the second exited state of iron at 2.085 MeV. This decay will still proceed, even if the iron is fully ionized. Therefore, for ionized cobalt, the half-life will be roughly a factor of 5 higher than for cobalt with two or more electrons. Recent data on cobalt-56 decay can be found in Junde (1999), Meyer (1990), Wang et al. (1988), and Bradley et al. (1986).

## 4. RESULTS: NICKEL DECAY IN $\gamma$-RAY BURST EJECTA

We now combine the physics of the previous two sections to describe the motion of the ionization front with the differing decay times of ionized and nonionized nickel and iron. We show that this produces unusual decay patterns that may be observable with an instrument such as the *Chandra X-Ray Observatory*.

The rate of change of the relative abundances of nickel-56, cobalt-56, and iron-56 is

$$\frac{dN_{\text{Ni}}}{dt} = -f_{\text{non}} \frac{N_{\text{Ni}}}{\tau_{\text{Ni}}} \ , \qquad (20)$$

$$\frac{dN_{\text{Co}}}{dt} = f_{\text{non}} \frac{N_{\text{Ni}}}{\tau_{\text{Ni}}} - f_{\text{non}} \frac{N_{\text{Co}}}{\tau_{\text{Co}}} - (1 - f_{\text{non}}) I_{\beta}^+ \frac{N_{\text{Co}}}{\tau_{\text{Co}}} \ , \qquad (21)$$

$$\frac{dN_{\text{Fe}}}{dt} = f_{\text{non}} \frac{N_{\text{Co}}}{\tau_{\text{Co}}} + (1 - f_{\text{non}}) I_{\beta}^+ \frac{N_{\text{Co}}}{\tau_{\text{Co}}} \ . \qquad (22)$$

Here $\tau_{\text{Ni}} = \tau_{1/2} \ln 2$ and $\tau_{1/2}$ is the half-life of nickel, and we use the similar relation for cobalt. Before the ionization front arrives, when $t < C_{f_\alpha} r_f^{3/(3-\alpha)}$, $C_{f_\alpha} = (C_{\text{rec}}/C_s)^{1/(3-\alpha)}$, the nonionized fraction is essentially unity. After the ionization front passes, the nonionized fraction is given by equation (9). We approximate the nonionized fractions of nickel, cobalt, and iron as the same. In reality, there will be slight quantitative differences since the ionization potential changes by roughly a keV from nickel to iron. How this difference translates into $f_{\text{non}}$ depends on the shape of the spectrum of the ionizing source.

We can solve the above equations approximately analytically to get the amount of nickel that remains as a function of time and also position in the ionization front. The general expression for the fraction of nickel remaining after the front has passed is

$$N(r_f, t) = \exp\left[-\frac{C_{f_\alpha} r_f^{3/(3-\alpha)}}{\tau_{Ni}}\right]$$
$$\times \exp\left[-\frac{C_{\text{non}}}{\tau_{\text{Ni}}} \int_{C_{f_\alpha} r_f^{3/(3-\alpha)}}^{t} \frac{dt}{C_{\text{non}} + t_d^{1-\alpha}}\right],$$
$$t_d > C_{f_\alpha} r_f^{3/(3-\alpha)} \ . \qquad (23)$$

Before the front has passed,

$$N(r_f, t) = \exp(-t_d/\tau_{Ni}), \ t_d < C_{f_\alpha} r_f^{3/(3-\alpha)} \ . \qquad (24)$$

For the special cases of $\alpha = 0$ and $\alpha = 1$, equation (23) becomes, for $\alpha = 0$,

$$N(r_f, t_d) \approx \exp\left(-\frac{C_{f_0} r_f}{\tau_{\text{Ni}}}\right) \left(\frac{C_{\text{non}} + t_d}{C_{\text{non}} + C_{f_0} r_f}\right)^{-C_{\text{non}}/\tau_{\text{Ni}}},$$
$$t_d > C_{f_0} r_f \qquad (25)$$

and for $\alpha = 1$,

$$N(r_f, t_d) \approx \exp\left(-\frac{C_{f_1} r_f^{3/2}}{\tau_{\text{Ni}}}\right) \exp\left[\frac{-f_{\text{non}}}{\tau_{\text{Ni}}}\left(t - C_{f_1} r_f^{3/2}\right)\right],$$
$$t_d > C_{f_1} r_f^{3/2} \qquad (26)$$

We show the results of our calculations in Figures 1 and 2. In Figures 1a and 1b, we show the fraction of nickel as a
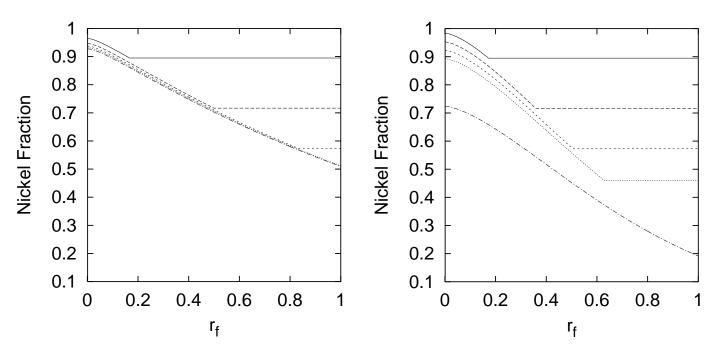
Fig. 1.—Fractional abundance of nickel as a function of position of the expanding material. *Horizontal axis*: Relative position, 0 nearest the ionizing source and 1 at the farthest edge. *Curves*: Different times since the initial ejection. Top curve is after one day, and the rest are, in descending order, 3, 5, 7, and 20 days. Ahead of the ionization front, the material decays normally, as seen by the horizontal lines. *Left panel*: Number of photons released from the ionizing source is constant as a function of time. *Right panel*: Ionizing source decays inversely with time, $\dot{N} \propto t_d^{-1}$.

function of position ($r_f$) in the ejected material for various times. One can see clearly the progress of the ionization front. Ahead of the front, there is a constant rate of decay as indicated by the horizontal line. Behind the front, the material is partially ionized, and this slows down the rate of decay. In the case where the flux from the accretion disk remains constant, the decay is much slower than in the case where the flux decreases as $t_d^{-1}$.

In Figure 2, we show the total fraction of nickel integrated over position. The lowest curve shows the amount of nickel as a function of time in the case of completely nonionized nickel. In the upper two curves, we show the change with rate of decay of the ionizing source.

In Figure 3, we show the amounts of nickel, cobalt, and iron as functions of time. We begin with relative abundances taken from Woosley & Weaver (1995), so that the iron-
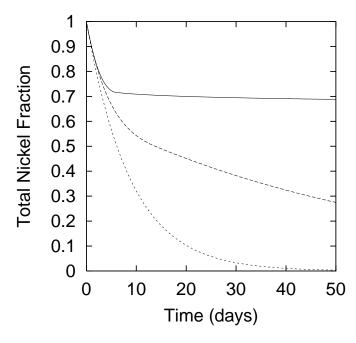


Fig. 2.—Total fractional amount of nickel in the ejected material as a function of time. *Top curve*: Constant ionizing source. *Middle curve*: Source that decays inversely with time, $\dot{N} \propto t_d^{-1}$. *Bottom curve*: Fraction of nickel in nonionized material.
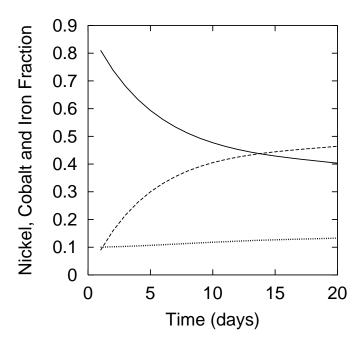
Fig. 3.—Total fractional amount of nickel (*solid line*), cobalt (*dashed line*), and iron (*dotted line*) as a function of time for the parameters given in the text and $\dot{N} \propto t_d^{-1}$.

group has roughly 90% nickel-56 and 10% iron. We then follow the decay at every point in the ejected material as the ionization front passes, and we integrate over position to look at the total amount of nickel, cobalt, and iron as functions of time. In these examples, the ionization front passes through the ejecta in 1–2 weeks. Strictly speaking, that poses a problem for seeing the iron-group emission lines reported in some afterglows within a day since it is presumed that we see $\gamma$-ray bursts along the direction of the funnel and the ejecta. In that case, we cannot see a significant line flux along the jet direction until the ionization front has passed through the ejecta. Real life, however, is likely to be more complex, with homogeneities in the ejecta and a dependence of properties on the distance to the jet axis, allowing the line photons to escape in some directions in some bursts. Alternatively, if the ejecta start out hot enough, as may be the case in a neutrino-driven disk wind, they may fully never recombine and always be more optically thin. Indeed, the lines are not seen in all afterglows and are seen only part of the time in those afterglows where they have been detected.

## 5. CONCLUSIONS

The astrophysical origin of $\gamma$-ray bursts remains a mystery even three decades after their discovery. However, technological advances in observing techniques have resulted in a great increase in data that are helping narrow down the possibilities. The recent observations of iron recombination lines in the X-ray afterglows of $\gamma$-ray bursts are an important clue to this problem.

Here we have discussed the importance of potentially observing the decay timscale of iron-group lines. The rate of decay will reflect the amount of time newly made nickel-56 has remained ionized. This information must then be interpreted in the context of the astrophysical site for $\gamma$-ray bursts.

We have suggested a model that has nickel-56 ejected from an accretion disk surrounding a black hole. Such a geometry is likely to exist at the center of a $\gamma$-ray burst. We have shown that the ejected material remains ionized due in part to the ionizing flux coming from the accretion disk. The degree of ionization depends on the parameters in the problem (such as the ejection velocity) and, importantly, the rate of decay of the flux coming from the accretion disk. We suggest that future observations of nickel, iron, and cobalt lines several days after the burst are an important test of this model. Since the decay of nickel-56 proceeds by electron capture, observation of a reduced rate of nickel decay would be a unique signal of ionization.

An interesting consequence of our model is that it would allow us to test for the presence of a hypernova even if we are observing it off-axis: as the ejected nickel is faster than the normal ejecta, it is always outside the general supernova material that explodes more isotropically. This implies that the X-ray line flux from the volume behind the ionization front will be scattered more or less isotropically and be observable from all directions. We can estimate the redshift out to which such a scattered flux would be visible by noting that the direct flux from the lines is detectable out to $z \simeq 1$. As long as the ionization front has not passed through the matter, a fraction of order unity of the direct flux will be scattered, and it will be roughly isotropic after scattering. This means that the flux toward any off-axis observer will be reduced by a factor $4\pi/\Omega_{jet} \sim 30$ relative to the line flux for an observer with a viewing direction within the jet. The distance out to which we can see the scattered flux is less than the maximum distance for the direct flux by the square root of that factor, i.e., it corresponds to $z \sim 0.2$. For much closer hypernova suspects (out to a few Mpc distance), even the $\gamma$-ray flux from the decaying nuclei could be observed with the *International Gamma-Ray Astrophysical Laboratory*. In both cases, detection would imply a very unusual event, likely a hypernova, since normally the iron-group elements produced in a supernova remain deeply hidden in the ejecta for a long time before the overlying layers become optically thin.

If we were to make observations of delayed nickel decay, it would lend support to the collapsar model of $\gamma$-ray bursts. Since most of the light from the $\gamma$-ray bursts comes in the $\gamma$-rays and in the afterglow, the central engine is difficult to observe. The type of recombination lines predicted here would, if observed, be a unique window into the center of the $\gamma$-ray burst.

## REFERENCES

Antonelli, L. A., et al. 2000, ApJ, 545, L39
Bloom, J. S., Sigurdsson, S., & Pols, O. R. 1999, MNRAS, 305, 763
Bradley, D. I., Stone, N. J., Rikovska, J., Novakova, D., & Ferencei, J. 1986, J. Phys. G, 12, 115
Brown, G. E., Lee, C.-H., Wijers, R. A. M. J., Lee, H.-K., Israelian, G., Bethe, H. A. 2000, NewA, 5, 191
Bulik, T., Belczynski, K., & Zbijewski, W. 1999, A&AS, 138, 483
Costa, E., et al. 1997, Nature, 387, 783
Dalal, N., Griest, K., & Pruet, J. 2002, ApJ, 564, 209
Eichler, D., Livio, M., Piran, T., & Schramm, D. N. 1989, Nature, 340, 126
Fisker, J. L., Martinez-Pinedo, G., & Langanke, K. 1999, European J. Phys., 5, 229
Frail, D. A., Kulkarni, S. R., Nicastro, L., Feroci, M., & Taylor, G. B. 1997, Nature, 389, 261
Frail, D. A., et al. 2001, ApJ, 562, L55
Janka, H.-Th., Eberl, T., Ruffert, M., & Fryer, C. 1999, ApJ, 527, L39
Junde, H. 1999, Nucl. Data Sheets, 86, 315
Kallman, T. R., Mészáros, P., & Rees, M. J. 2002, ApJ, submitted (astro-ph/0110654)
Lang, K. 1980, Astrophysical Formulae: A Compendium for the Physicist and Astrophysicist (Berlin: Springer)
MacFadyen, A. I. 2002, Gamma-Ray Burst Progenitors: the Collapsar Model
MacFadyen, A. I., & Woosley, S. E. 1999, ApJ, 524, 262

McLaughlin, G. C., Wijers, R. A. M. J., Brown, G. E., & Bethe, H. A. 2002, ApJ, 564, 454
Mészáros, P., & Rees, M. J. 1997, ApJ, 476, 232
Mészáros, P., Rees, M. J., & Wijers, R. A. M. J. 1999, NewA, 4, 303
Metzger, M. R., Djorgovski, S. G., Kulkarni, S. R., Steidel, C. C., Adelberger, K. L., Frail, D. A., Costa, E., & Frontera, F. 1997, Nature, 387, 879
Meyer, R. A. 1990, Nucl. Data Sheets, 22, 153
Mochkovitch, R., Hernanz, M., Isern, J., & Martin, X. 1993, Nature, 361, 236
Paczyński, B. 1998, ApJ, 494, L45
Panaitescu, A., & Kumar, P. 2001, ApJ, 560, L49
Piran, T. 1999, Phys. Rep., 314, 575
Piro, L., et al. 1999, ApJ, 514, L73
———. 2000, Science, 290, 955
Rees, M. J., & Mészáros, P. 1992, MNRAS, 258, L41
———. 2000, ApJ, 545, L73
Reeves, J. N., et al. 2002, Nature, 416, 512
Ruffert, M., & Janka, H.-T. 1999, A&A, 344, 573
Salmonson, J. D., Wilson, J. R., & Mathews, G. W. 2001, ApJ, 553, 471
Sur, B., Norman, E. B., Lesko, K. T., Browne, E., & Larimer, R. M. 1990, Phys. Rev. C, 42, 573
van den Berk, D. E., et al. 2002, ApJ, submitted (astro-ph/0111054)
van Paradijs, J., Kouveliotou, C., & Wijers, R. A. M. J. 2000, ARA&A, 38, 381

van Paradijs, J., et al. 1997, Nature, 386, 686
Vietri, M., Ghisellini, G., Lazzati, D., Fiore, F., & Stella, L. 2001, ApJ, 550, L43
Vreeswijk, P. M., et al. 2002, MNRAS, submitted
Wang, G., Warburton, E. K., & Alburger, D. A. 1988, Nucl. Instrum. Methods Phys. Res., 272, 791

Weth, C., Mészáros, P., Kallman, T., & Rees, M. J. 2000, ApJ, 534, 581
Wijers, R. A. M. J., Rees, M. J., & Mészáros, P. 1997, MNRAS, 288, L51
Woosley, S. E. 1993, ApJ, 405, 273
Woosley, S. E. & Weaver, T. A. 1995, ApJS, 101, 181